Technical Note

Rock Mass Erodibility

Steven E. Pells, Ph.D.[1]; Kurt Douglas, Ph.D.[2]; Philip J. N. Pells, D.Sc., M.ASCE[3]; Robin Fell[4]; and William L. Peirson, Ph.D.[5]

Abstract: Erosion of rock masses by water typically involves unraveling of blocks of rock along existing defects in a manner that is not represented by analytical solutions for sediment transport or rockfill (rip-rap). A pragmatic approach to this complex problem is found by using a rock mass index to represent the erodibility of the rock-mass. The likelihood of erosion is then assessed by comparison against case studies in similar rock masses. A new independent data set of rock-mass erosion was gained from inspection of 26 unlined spillways in Australia, South Africa, and the United States. It was found that erosion can be usefully correlated against various published rock mass indices and hydraulic indices. A modified rock mass index, developed specifically to represent erodibility, is presented, and is applied to prepare a new comparative erosion assessment method for rock masses. **DOI: 10.1061/(ASCE)HY.1943-7900.0001243.**

Author keywords: Erosion; Scour; Rock; Fractured rock; Blocky rock; Jointed rock; Rock mass index; Erodibility; Stream power; Spillways.

Introduction

Rock masses are complex geological structures that, over a broad scale, have engineering properties that are heterogeneous and difficult to measure. Rapid erosion (or "scour") of rock masses by water involves dismantling this complex structure by equally complex fluctuating hydraulic pressures. Dramatic and unexpected erosion of high strength and quite massive rock has impacted the safe operation and maintenance costs of spillways of several major dams (i.e., Fig. 1).

Erosion assessment methods for soils or placed rockfill are numerous, but are not applicable to rock masses. Rock mass characteristics are unique to each site and involve a degree of complexity such that a generalized analytical model of erosion of fractured rock masses is neither achievable nor appropriate.

A pragmatic approach is to use a rock mass index to represent rock-mass erodibility. Erodibility of a particular rock mass is then assessed by comparison to the performance of case studies with similar rock mass index values. This comparative approach has enjoyed wide usage in dam spillway assessments (USSD 2006).

Existing comparative design methods are reviewed subsequently. Using new data from investigations of 26 dam spillways in Australia, South Africa, and the United States, a new rock mass index is developed to represent erodibility of rock masses and offer a range of advantages over past techniques.

[1]Associate, Pells Consulting, 49 Lakeside Dr., MacMasters Beach, NSW 2251, Australia (corresponding author). ORCID: http://orcid.org/0000-0002-3220-0707. E-mail: steven@pellsconsulting.com.au

[2]Senior Lecturer, School of Civil and Environmental Engineering, UNSW Australia, Sydney, NSW 2052, Australia.

[3]Director, Pells Consulting, 49 Lakeside Dr., MacMasters Beach, NSW 2251, Australia; Adjunct Professor, UNSW Australia, Sydney, NSW 2052, Australia.

[4]Emeritus Professor, UNSW Australia, Sydney, NSW 2052, Australia.

[5]Director, Water Research Laboratory, School of Civil and Environmental Engineering, UNSW Australia, King St., Manly Vale, NSW 2052, Australia.

Note. This manuscript was submitted on December 12, 2015; approved on July 12, 2016; published online on November 29, 2016. Discussion period open until April 29, 2017; separate discussions must be submitted for individual papers. This technical note is part of the ***Journal of Hydraulic Engineering***, © ASCE, ISSN 0733-9429.

Review of the Use of Rock Mass Indices in Representing Rock Mass Erodibility

Starfield and Cundall (1988) described rock mechanics problems as "data-limited problems," reflecting the difficulty in characterizing rock masses because of heterogeneity in size, shape, orientation, and strength. In the 1970s, engineering rock-mass classification systems were developed that sought to characterize a rock mass with a single index based on selected rock-mass qualities such as rock strength, joint characteristics, and groundwater conditions. The rock mass rating (*RMR*) system of Bieniawski (1973) and the *Q*-system (*Q*) of Barton et al. (1974) are now used worldwide for diverse design considerations ranging from tunnel support to foundations and open pit slope faces. Rock mass index uses and limitations are discussed in standard texts (e.g., Hoek and Brown 1980; Hudson and Harrison 2005), including cautions against over-reliance on indices in lieu of proper geological investigation and engineering design (Pells 2008).

Rock mass indices have been developed for specific applications such as "rippability," which is the ease with which soil or rock can be mechanically excavated [MacGregor et al. (1994) listed 11 rippability index methods]. Moore and Kirsten (1988) proposed that erosion of rock is similar to excavation of rock by ripping and that a published rock mass index of rippability (Kirsten 1982) could represent the erodibility of materials. Moore et al. (1994) reinterpreted the geology at case studies of spillway erosion documented in Moore (1991) (primarily in soils and soft rock) in terms of the Kirsten rippability index *K*; the flow conditions causing erosion were characterized using the stream power dissipation, and a threshold between eroding and noneroding conditions was interpreted.

Erosion within spillways of over 30 dams in South Africa, primarily in fractured rock environments, was investigated by Pitsiou (1990) and Dooge (1993). In van Schalkwyk et al. (1994a, b), data from 18 of these dams were presented, with the unit stream power dissipation Π_{UD} [Eq. (1)] used to characterize hydraulic loading; *K* to characterize the geology; and the observed erosion qualitatively categorized as "none," "some," or "excessive." van Schalkwyk (1994) subsequently updated the findings by including the case study data from Moore (1991)

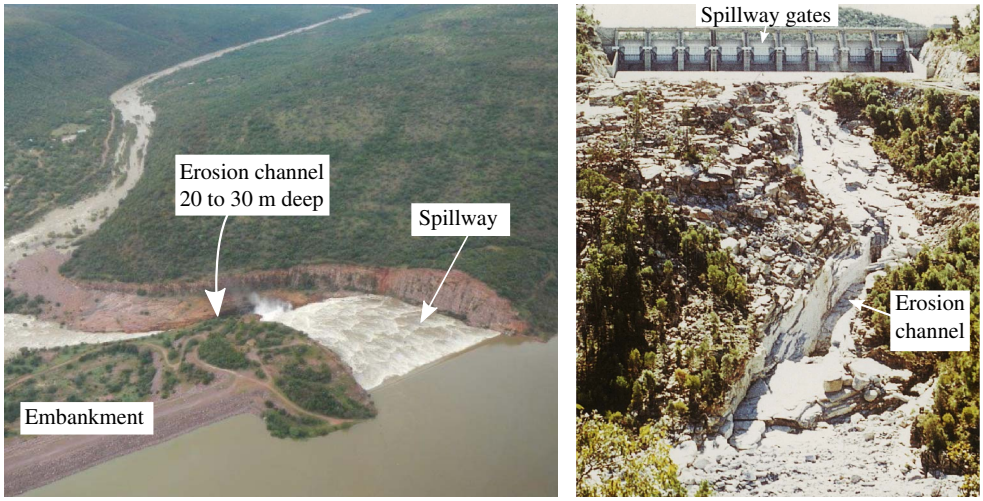

Fig. 1. (a) Erosion at Mokolo dam, South Africa (courtesy of Walther van der Westhuizen); (b) Copeton dam, Australia (courtesy of WaterNSW)

$$\Pi_{UD} = \rho g q \frac{dE}{dx} \tag{1}$$

Π_{UD} = dissipation of hydromechanical energy per unit area ($W \cdot m^{-2}$); ρ = density of water ($kg \cdot m^{-3}$); g = acceleration due to gravity ($m \cdot s^{-2}$); and dE/dx = total energy head (m) expended per meter length (equivalent to the slope of the total energy line, the friction slope S_f).

Annandale (1995) supplemented the data sets used by Moore et al. (1994) and van Schalkwyk et al. (1994b) with data from Bartlett Dam, Arizona, "published data on incipient motion of noncohesive earth materials" (Annandale 2005, p. 221), and presented, again, the data as a plot of Π_{UD} versus K, finding an alternative curve to demarcate between eroding and noneroding conditions. Annandale (1995) renamed the Kirsten index the "erodibility index," but used the Kirsten index without modification.

Kirsten (1995) argued that the relationship between K and Π_{UD} could also represent the erodibility of other (nonearth) materials and compiled a data set of erosion of materials ranging from fine sediment to intact steel (K ranging over 21 log cycles). For dam spillways, Kirsten et al. (2000) prepared a plot of Π_{UD} versus K based on the data from Moore (1991) and Dooge (1993), finding a curve to demarcate between eroding and noneroding conditions.

Interpreted scour thresholds from the previously cited authors are summarized in Fig. 2. The curves in Fig. 2 were presented by the respective authors as a design method: initiation of scour could be judged by comparing how a site-specific determination of Π_{UD} and K plots relative to the curves.

The designer, however, is confronted with a problem: Which curve to use? Why were such diverse scour thresholds interpreted, particularly when each curve was based primarily on the same data sets (for rock) of Moore (1991) and Dooge (1993)? A detailed review of the interpreted curves, including inspection of many of the spillways in South Africa, was presented in Pells et al. (2015a, 2016), finding that

1. The data sets of van Schalkwyk (1994) and Annandale (1995) share no common data points despite referencing the same case data, indicating reinterpretation of Π_{UD}, K, and the amount of erosion. Subject to re-interpretation, the data presented by Annandale (1995) cluster around an interpreted threshold, whereas the data presented by van Schalkwyk (1994) show considerable scatter. No further site investigations had been undertaken (van Schalkwyk, personal communication, 2014; Kirsten et al., personal communication, 2014); hence the basis for re-interpretation of K and the amount of erosion is unknown.
2. Hydraulic analysis presented in van Schalkwyk et al. (1994a) and Kirsten et al. (2000) assumed uniform flow conditions (i.e., $\Pi_{UD} = \rho g q S_f$, where $S_f = S_o$). For plunging flow conditions, van Schalkwyk et al. (1994b) assumed that $S_f = 3$. Annandale (1995) presented analytical solutions for some idealized nonuniform flow scenarios (e.g., Knickpoints, hydraulic jumps, and plunging conditions), but neglected the length over which dissipation occurred, requiring $dx = 1$ m for dimensional consistency, resulting in significant overestimation of Π_{UD}. Analytical estimates of Π_{UD} were shown by Pells (2016) to generally have high uncertainty.
3. Detailed topographic survey data from before and after an event were typically unavailable, requiring subjective interpretation of the erosion amount. Based on investigation of case sites, it was considered inappropriate to characterize field observations according to the binary paradigm of eroding and noneroding.
4. A blind test study by P. J. N. Pells et al. "RQD—Time to rest in peace," submitted, *Can. Geotech. J.*, Ottawa, Ontario, Canada, showed large discrepancies should be expected in estimation of K, even between experienced practitioners. In

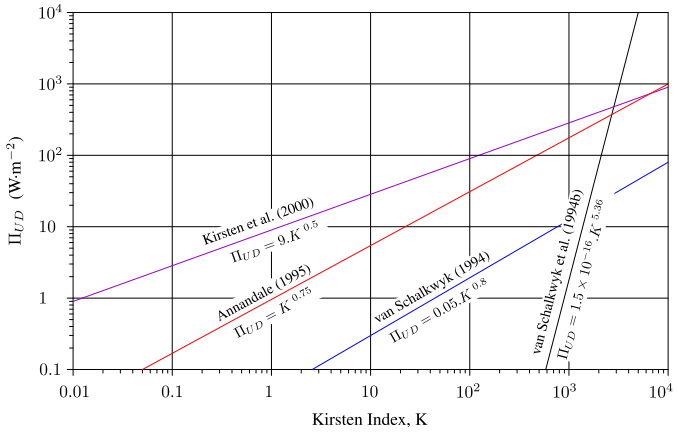

Fig. 2. Scour thresholds, various authors

particular, the RQD parameter used in the Kirsten index was found to be a source of error arising from indirect estimation practices that depart from the original intent of Deere (1962).
5. An independent data set of Π_{UD} versus K gained by Pells (2016) did not favor either of the published thresholds, but rather showed a gradation. With respect to data uncertainty and the observed nature of erosion in spillways, it was considered physically and statistically unlikely that a binary scour threshold should arise from the data.
6. van Schalkwyk et al. (1994a) interpreted the scattered data into regions of erosion extent rather than a threshold. These regions were found to be compatible with the independent data set presented in Pells (2016).

Comments on Hydraulic Indices to Represent Erosive Power

Kirsten and Kirsten (1995) and Kirsten et al. (2000) argued Π_{UD} is an appropriate index of erosive capacity because it is correlated to turbulence intensity, and Annandale (1995) presented laboratory data correlating Π_{UD} to the magnitude of pressure fluctuations within a hydraulic jump. Such a correlation was validated by laboratory data presented in Pells (2016), although it was shown that the correlation applies equally to $\bar{\tau}_o$ and also somewhat to $\bar{u}$ ($\bar{\tau}_o \propto \bar{u}^2$ and $\Pi_{UD} \propto \bar{u}^3$).

Dissipation of hydraulic power is primarily due to heat conversion, not on work done in moving bed particles; hence Π_{UD} is not a direct measure of erosive capacity. Similarly, $\bar{\tau}_o$ is a physical measure of normal stress applied to the bed, which is only a component of the erosive process. The mean flow velocity $\bar{u}$ relates directly to the stagnation pressures that can form against a face of a rock or within defects—such differential pressures on opposing faces of a rock element are a key process for erosion of fractured rock. The indices all suffer from nonuniqueness in their representation of flow conditions—there is an infinite combination of spillway geometry and discharge that can be associated with a given measure of Π_{UD}, $\bar{\tau}_o$, or $\bar{u}$.

In the absence of detailed flow data, these hydraulic indices are calculated for case studies using the peak discharge from the flood of record. This assumes hydraulic conditions at the peak of the hydrograph are representative of the entire flood event. Clearly, not all hydrographs are equal, and they can vary significantly in duration. An estimation of the total energy expenditure over selected flood hydrographs by Pells (2016) found that the peak Π_{UD} was only broadly correlated to the hydraulic erosive power experienced by a spillway over a spill event and is appropriate as an indicator for the purposes of comparison only.

Case Study Investigations

A study program was undertaken in which erosion at 26 case study sites was examined, providing 118 data points of erosion, almost exclusively within fractured rock environments. The case studies included spillways that had suffered significant erosion, but also spillways that had largely resisted erosion despite having endured large flood events. Data from two dams in the United States were gained from review of published literature only. The data from case studies in Australia (14 dams) and South Africa (10 dams) were based on site inspections undertaken by the authors.

For each spillway, a review of published and privately owned data relevant to the site was undertaken, including geological mapping, site testing, construction records, photographs, previous geotechnical site investigations, and spillway flow or reservoir level data. Geological domains and key structural features (e.g., faults, dykes) were identified on each spillway. Examination areas, regions of interest to erosion, were then visually identified, where rock mass properties could be readily examined and where erosion had occurred or failed to develop in earnest despite significant hydraulic loading. A visual classification of the extent of erosion was made based on observed erosion depth and extent according to the five classes presented in Table 1. Geological field procedures assessed the rock substance and rock mass properties, including defect orientation and spacing relevant to each erosion area. The factual information recorded from this methodology was documented into separate reports for the Australian, South African, and United States cases (Pells 2016). As an independent process, interpretation of selected rock mass indices for each of the erosion areas was then undertaken based on the documented factual information.

Table 1. Erosion Classes

Maximum depth (m)	General extent (m^3 per 100 m^2)	Class	Descriptor
<0.3	<10	I	Negligible
0.3–1	10–30	II	Minor
1–2	30–100	III	Moderate
2–7	100–350	IV	Large
>7	>350	V	Extensive

The peak discharge Q ($m^3 \cdot s^{-1}$) for each site was obtained from historical records and was used to calculate $\bar{u}$, $\bar{\tau}_o$, and Π_{UD} at each of the identified examination areas using a combination of analytical hand calculations and one-dimensional numerical modeling using HEC-RAS (USACE Hydrologic Engineering Centre 2010). The numerical modeling provided a more detailed view of the slope of the total energy line S_f in the context of changing channel width, slope, and roughness that were characteristic of the study sites. The numerical model also reported the total energy upstream and downstream of prominent features such as drops and hydraulic jumps, from which an assessment of energy slope over the feature was made. HEC-RAS reported the total energy at the upstream and downstream extents of hydraulic jumps, but was found not to produce a reliable estimate of the length of the jump (the reported length was a function of the computational spacing). In such instances, the jump length was taken as $6y_2$, where y_2 = water depth downstream of the jump (after Henderson 1966). Because the rate of energy dissipation over the jump may not be linear, an upper bound estimate of the friction slope over the jump was also made, assuming 80% of the energy was lost over the first 50% of the jump length. Only in some cases, where limited topographic data was available, were analytical estimates preferred to the HEC-RAS output. Classical analytical representations of nonuniform flow scenarios such as headcuts, hydraulic jumps, and Knickpoints relate to idealized flow geometry and backwater conditions, and were found to be rarely applicable to real-world case data.

Rock Mass Erodibility Index

The data set compiled from the case study investigations was used to investigate alternative or improved representations of rock mass erodibility, as described subsequently.

Representation of Erodibility Using Existing Rock Mass Indices

An index of erodibility based on the Q or RMR indices, rather than K, would align with current engineering geology practice. The RMR parameter for discontinuity orientation adjustment (Bieniawski 1973) is specific to slope and tunnel engineering

and is not applicable to erodibility. A rock mass index that employs *RMR* without the discontinuity orientation adjustment has already been developed and published as the geological strength index (*GSI*) (Hoek et al. 1995). In the early 2000s, various charts were published that provided a simple and visual means of directly estimating *GSI* for various rock types (e.g., Marinos and Hoek 2000, 2001). An example of such a chart for jointed rocks is presented in Fig. 3. Although the chart was originally conceived as an accessible means to estimate *GSI*, it has, over time, taken on an authority of its own. Hoek (2006, Chapter "Rock mass properties," p. 12) recommended that the chart, rather than *RMR* values, should be used to estimate *GSI*.

Q' values (Barton et al. 1974, with an active stress number of unity) and *GSI* values were assessed for each of the 118 case study examination areas. Plots presented in Pells (2016) showed that both *GSI* and Q' could be usefully correlated against erosion. The Kirsten modification of Q to represent rippability using M_S and J_S did not result in improved representation of erodibility of fractured rock.

The M_S number for rocks is tabulated in Kirsten (1982) as a step function of the unconfined compressive strength (UCS) of the rock substance. A fundamental aspect of rock mechanics is the demarcation of rock *substance* strength (strength of an intact sample) and rock *mass* strength (strength of a mass, including defects). The

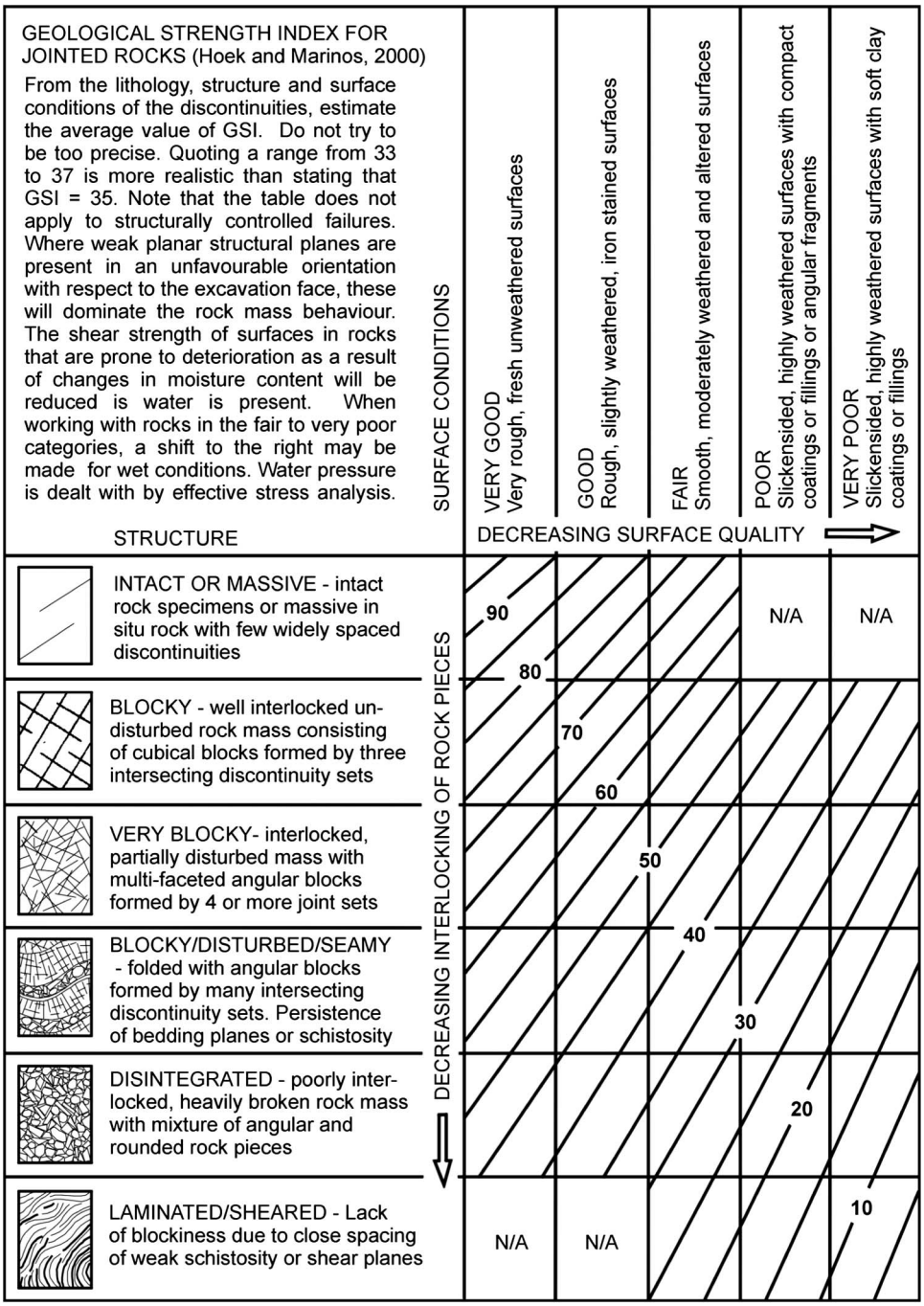

Fig. 3. Chart for characterization of GSI of blocky rock masses on the basis of interlocking and joint conditions (reprinted from Hoek 2006, with permission)

J. Hydraul. Eng., 2017, 143(5): 06016031

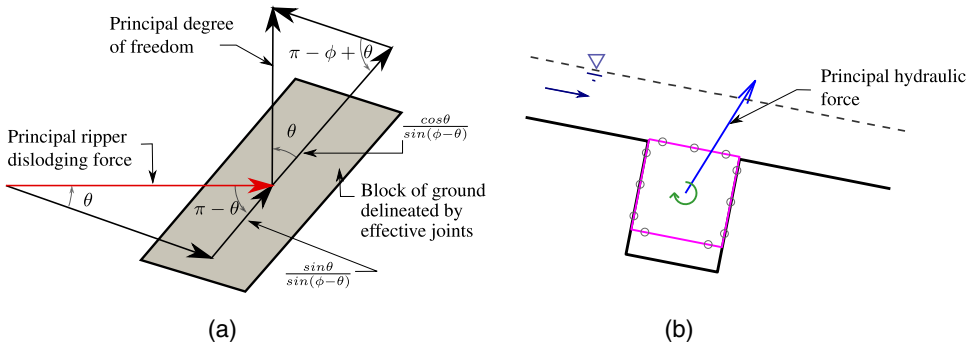

Fig. 4. (a) Free body presented for derivation of J_s (adapted from Kirsten 1982) versus (b) example of principal hydraulic force (reprinted from Pells 2016)

process of erosion of fractured rock is observed to comprise unraveling of blocks of rock along existing defect lines, rather than breakdown of the rock substance as might occur during ripping. It is thus believed that rock *substance* strength plays a very limited role in the erodibility of fractured rock masses. In contrast, the value of K is strongly dominated by the M_S value.

The J_s number represents the relative orientation and spacing of defects that "affect the effort required to penetrate the ground as well as the effort required to dislodge individual blocks" (Kirsten 1982, p. 300). Kirsten (1982) derived a mathematical expression to represent vulnerability of a rock mass to such penetration and dislodgement by the tine of an excavator or ripper. The J_s number has been applied to erodibility simply by substituting the flow direction for the ripping direction (e.g., van Schalkwyk et al. 1994a; Annandale 1995; Kirsten et al. 2000). The kinematics used by Kirsten (1982) to derive J_S are based on a principal dislodging force that is parallel to the slope and acts in the downstream direction (Fig. 4(a), left). Hydraulic testing presented in Pells (2016) showed that the principal force on an element from hydraulic loading varies considerably, with a strong vertical component likely to be present (Fig. 4(b), right). In some circumstances, the principal force may even have an upstream direction. It is also considered that the probability of a point-specific excavator tine striking a defect is not representative of vulnerability to a spatially distributed hydraulic pressure. Hence, although defect orientation is agreed to be an important aspect of erodibility, it is considered that the J_s number, as developed for rippability, is not representative of erodibility.

New Index of Rock Mass Erodibility

The observed correlation between erosion and *GSI* index was of particular interest because the *GSI* chart is perceived to pictorially represent key aspects of erodibility without being dominated by a substance strength value or encumbered with the problematic *RQD* parameter (P. J. N. Pells et al. "RQD—Time to rest in peace," submitted, *Can. Geotech. J.*, Ottawa, Ontario, Canada). It also has a number of operational advantages: values obtained from the *GSI* chart (Fig. 3) are substantially easier to obtain and have an established and endorsed understanding in engineering geology practice. It is also considered that the *GSI* chart, by using a pictorial method, provides an appropriate inference of accuracy—the practitioner is forced to consider that geological structure, then consciously apply a simplification to obtain an index of the rock quality. In contrast, mathematical operation on a number of parameters may provide an unjustified inference that an accurate model of the rock structure is being obtained through calculation. There was also evidence in P. J. N. Pells et al. "RQD—Time to rest in peace," submitted, *Can. Geotech. J.*, Ottawa, Ontario, Canada, and Bertuzzi et al. (2016) that the *GSI* chart resulted in more consistent interpretations between practitioners, particularly those with less experience in engineering geology. This is of considerable importance because erosion assessments may be undertaken by hydraulics practitioners.

However, *GSI* values do not represent vulnerability to erosion from unfavorable orientation of defects. A new discontinuity orientation adjustment representing erodibility was thus proposed

$$eGSI = \max \begin{cases} GSI + E_{doa} \\ 0 \end{cases} \tag{2}$$

$eGSI$ = rock mass erodibility index and E_{doa} = discontinuity orientation adjustment for erodibility.

Eq. (2) takes the form of the original *RMR* equation (Bieniawski 1973). The erodibility index has nonetheless been termed *eGSI* rather than *eRMR* because it is recommended that the value of *GSI* in Eq. (2) be obtained from Fig. 3 rather than by calculation from the *RMR* components.

The proposed values of E_{doa} are presented in Figs. 5 and 6. Various pictograms were drawn of rock masses with two orthogonal joint sets at various orientations relative to the direction of flow and with various relative spacings. For the pictograms, the surface was considered to be defined primarily along defect lines, as observed at spillway sites. The surface formed in this way creates a roughness and shape that reflect the joint structure. The E_{doa} values were derived by assessing the vulnerability to significant and ongoing erosion, taking into consideration the kinematics of block removal and the nature and direction of hydraulic loading, as observed at case studies and in model tests presented in Pells (2016). Pictograms were repeated for various hydraulic loading configurations. The process was also undertaken for nonorthogonal joint sets, but the appraised values were not significantly different. The pictograms presented in Figs. 5 and 6 were selected as sufficiently representative of the case studies investigated.

A plot of Π_{UD} versus the *eGSI* index presented in Pells (2016) demonstrated that the inclusion of the factor E_{doa} provided an improved correlation to erosion. Erosion classes were then contoured manually with consideration to each data point (Fig. 7) and allowing for the expected nature of error bars. These contours considered that as *eGSI* approaches 100, defects would become of negligible influence to erodibility, and erosion could proceed only through breakdown of the rock substance. A value of 1×10^5 to 1×10^6 kW · m^{-2} was used to represent the onset of erosion of the rock substance based on stream power required for jet-cutting of rock, as presented in Kirsten (1995). For small values of *eGSI*, there is some evidence from the data that erosion becomes increasingly controlled by the nature of the rock, rather than hydraulic loading, and the interpreted

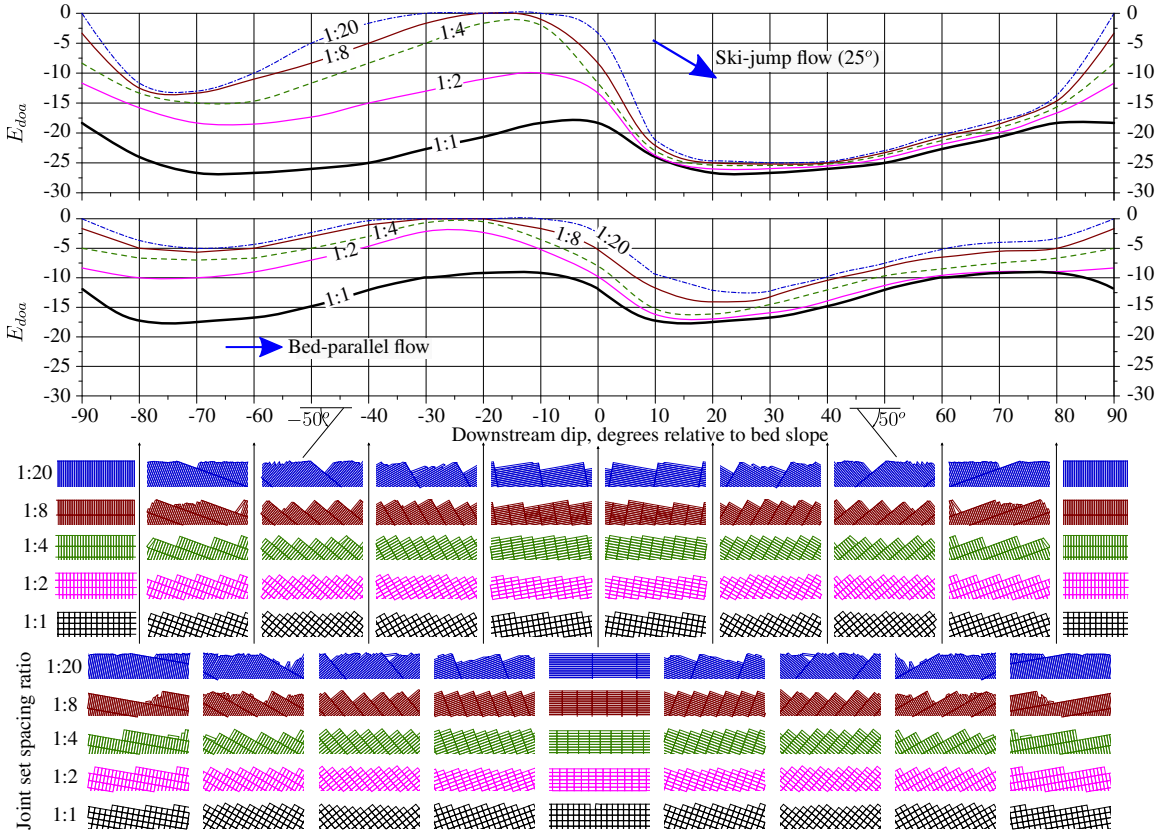

Fig. 5. Discontinuity orientation adjustment for erosion (E_{doa}) for horizontal beds

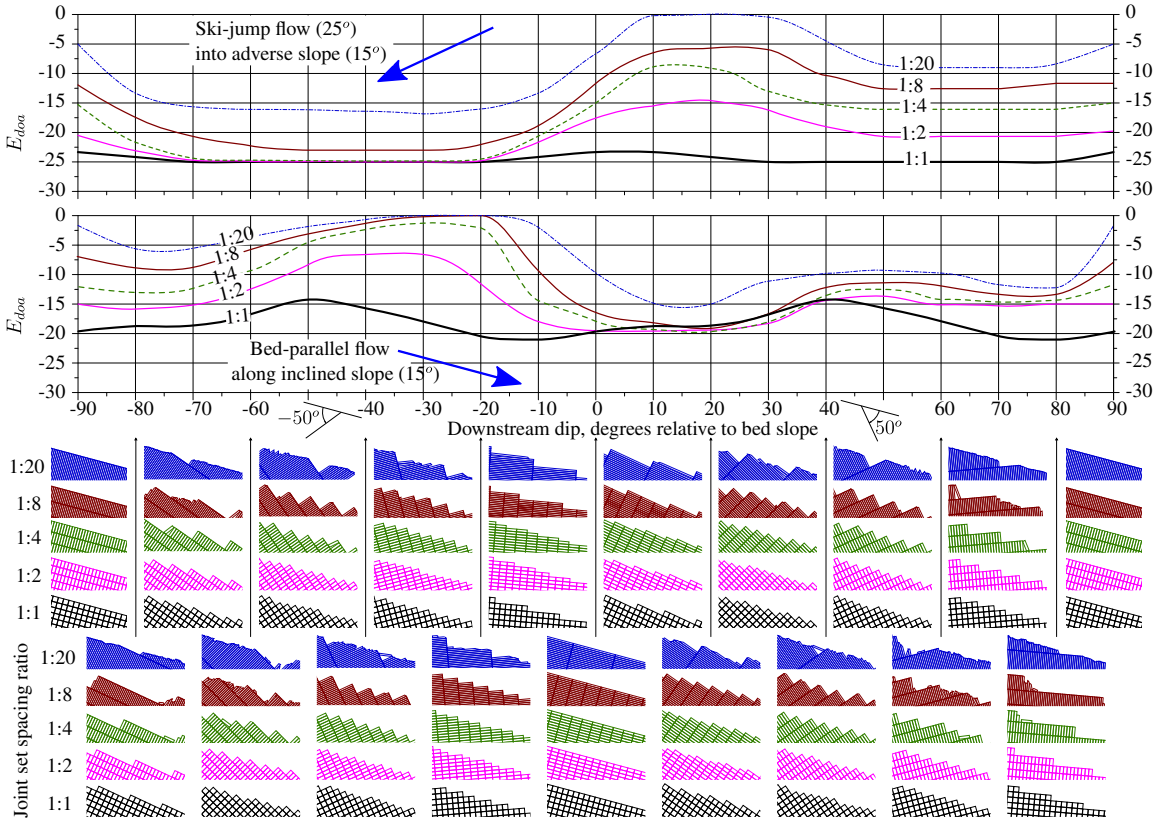

Fig. 6. Discontinuity orientation adjustment for erosion (E_{doa}) for inclined beds

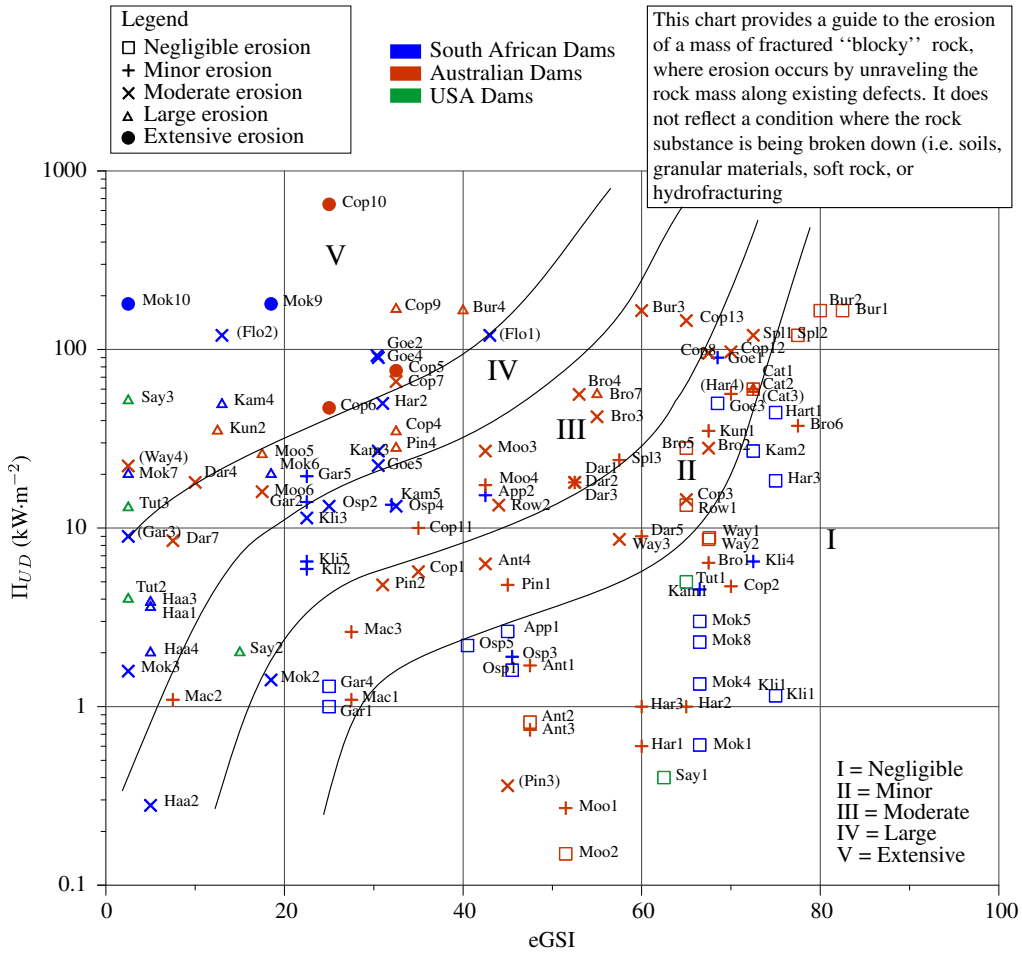

Fig. 7. Interpreted erosion categories—unit stream power dissipation versus *eGSI*

classes were drawn to reflect this. A plot of $\bar{\tau}_o$ versus the *eGSI* index was similarly developed (presented in Pells 2016).

Summary

The 118 data points gained from 26 spillways in Australia, South Africa, and the United States have been used to demonstrate that a useful correlation can be found between various rock mass indices, various hydraulic indices, and observed erosion. The correlation can be capitalized upon to obtain an indication of erosion risk.

A new index of rock mass erodibility was presented. The erodibility index is determined using Figs. 5 or 6 and 3. The assessment of erosion risk is undertaken with reference to Fig. 7, supported by calculation of Π_{UD}. This method is applicable to fractured rock environments experiencing unit stream power dissipation of up to 1000 kW · m^{-2} and is considered preferable to existing published erodibility methods because it is underpinned by a more comprehensive and transparent data set from fractured rock environments—the labeled data points can also be readily traced to detailed case studies presented in Pells (2016). The advantages gained from usage of *GSI* are described previously, and include ease of use, established credibility, improved consistency of interpretation, and appropriate inference of accuracy.

When making an assessment of this nature, the practitioner is simply benchmarking the site in question against erosion observed at case studies of unlined dam spillways in rock. Rock mass indices are simplistic representations of a rock mass, and Π_{UD} is an approximate indicator of erosive power. This method is therefore useful for initial and comparative assessments, and does not constitute modeling of the erosion detachment process.

Notation

The following symbols are used in this paper:

E = hydraulic energy (m);
E_{doa} = discontinuity orientation adjustment for erodibility;
eGSI = geological strength index, modified for erodibility;
GSI = geological strength index, after Hoek et al. (1995);
g = acceleration due to gravity (m · s^{-2});
K = rock mass index for rippability, after Kirsten (1982);
Q = discharge (m^3 · s^{-1});
Q = rock mass quality index, after Barton et al. (1974);
q = unit discharge (m^2 · s^{-1});
RMR = rock mass rating, after Bieniawski (1973);
RQD = rock quality designation, after Deere (1962);
$\bar{u}$ = average cross-sectional flow velocity (m · s^{-1});
Π_{UD} = unit stream power dissipation (W · m^{-2});
ρ = density of water (kg · m^{-3}); and
$\bar{\tau}_o$ = average bed shear stress (Pa).

References

Annandale, G. W. (1995). "Erodibility." *J. Hydraul. Res.*, 33(4), 471–494.

Annandale, G. W. (2005). *Scour technology: Mechanics and engineering practice*, 1st Ed., McGraw-Hill Professional, New York.
Barton, N., Lien, R., and Lunde, J. (1974). "Engineering classification of rock masses for the design of tunnel support." *Rock Mech.*, 6(4), 189–236.
Bertuzzi, R., Douglas, K., and Mostyn, G. (2016). "Comparison of quantified and chart GSI for four rock masses." *Eng. Geol.*, 202, 24–35.
Bieniawski, Z. T. (1973). "Engineering classification of jointed rock masses." *Civ. Eng. South Afr.*, 15(12), 335–344.
Deere, D. U. (1962). *Technical description of rock cores for engineering purposes*, Univ. of Illinois, Champaign, IL.
Dooge, N. (1993). "Die hidrouliese erodeerbaarheid van rotmassas in onbelynde oorlope met spesiale verwysing na die rol van naatvulmateriaal." M.Sc. thesis, Univ. of Pretoria, South Africa (in Afrikaans).
Henderson, F. (1966). *Open channel flow*, 1st Ed., Prentice Hall, Upper Saddle River, NJ.
Hoek, E. (2006). "Practical rock engineering." ⟨https://www.rocscience.com/hoek/corner/Practical_rock_engineering.pdf⟩ (Jun. 4, 2015).
Hoek, E., and Brown, E. T. (1980). *Underground excavations in rock*, Institution of Mining and Metallurgy, London.
Hoek, E., Kaiser, P. K., and Bawden, W. F. (1995). *Support of underground excavations in hard rock*, A.A. Balkema, Rotterdam, Netherlands.
Hudson, J. A., and Harrison, J. P. (2005). *Engineering rock mechanics: An introduction to the principles*, Pergamon, Tarrytown, NY.
Kirsten, H. (1982). "Classification system for excavation in natural materials." *Civ. Eng. South Afr.*, 24(7), 293–308.
Kirsten, H. (1995). "Erodibility criterion for jet cutting of intact materials." *Rep. 197083/3*, Steffen, Robertson, and Kirsten Incorporated, Johannesburg, South Africa.
Kirsten, H., and Kirsten, L. (1995). "Stream power as a measure of excitation causing hydraulic erosion." *Rep. No. 197083/2*, Stefan, Robertson, and Kirsten Incorporated, Johannesburg, South Africa.
Kirsten, H. A., Moore, J. S., Kirsten, L. H., and Temple, D. M. (2000). "Erodibility criterion for auxiliary spillways of dams." *Int. J. Sediment Res.*, 15(1), 93–107.
MacGregor, F., Fell, R., Mostyn, G. R., Hocking, G., and McNally, G. (1994). "The estimation of rock rippability." *Q. J. Eng. Geol. Hydrogeol.*, 27(2), 123–144.
Marinos, P. and Hoek, E. (2000). "GSI—A geologically friendly tool for rock mass strength estimation." *ISRM Int. Symp.*, International Society for Rock Mechanics, Melbourne, VIC, Australia.
Marinos, P., and Hoek, E. (2001). "Estimating the geotechnical properties of heterogeneous rock masses such as flysch." *Bull. Eng. Geol. Environ.*, 60(2), 85–92.
Moore, J. (1991). *The characterization of rock for hydraulic erodibility*, Water Resources Publications, Littleton, CO.
Moore, J., and Kirsten, H. (1988). *Discussion—Critique of the rock material classification procedure*, L. Kirkaldie, ed. ASTM, West Conshohocken, PA.
Moore, J. S., Temple, D. M., and Kirsten, H. (1994). "Headcut advance threshold in earth spillways." *Bull. Assoc. Eng. Geol.*, 31(2), 277–280.
Pells, P. J. N. (2008). "What happened to the mechanics in rock mechanics and the geology in engineering geology?" *South Afr. Inst. Min. Metall.*, 108, 309–323.
Pells, S. (2016). "Erosion of rock in spillways." Ph.D. thesis, UNSW Australia, Kensington, NSW, Australia.
Pells, S., Pells, P., Peirson, W. L., Douglas, K., and Fell, R. (2015a). "Erosion of unlined spillways in rock - does a 'scour threshold' exist?" ANCOLD, Brisbane, QLD, Australia.
Pitsiou, S. (1990). "The effect of discontinuities on the erodibility of rock in unlined spillways." M.Sc. thesis, Univ. of Pretoria, Pretoria, South Africa.
Starfield, A., and Cundall, P. (1988). "Towards a methodology for rock mechanics modelling." *Int. J. Rock Mech. Min. Sci. Geomech. Abstr.*, 25(3), 99–106.
USACE Hydrologic Engineering Centre. (2010). "HEC-RAS river analysis system hydraulic reference manual." *Computer program documentation version 4.1*, Davis, CA.
USSD (United States Society on Dams). (2006). "Erosion of unlined spillways." Denver.
van Schalkwyk, A. (1994). "Minutes—Erosion of rock in unlined spillways." *ICOLD*, Q.71-17, 1056–1062.
van Schalkwyk, A., Jordaan, J., and Dooge, N. (1994a). "Die erodeerbaarheid van verskillende rotsformasies onder varierende vloeitoestande." *Rep. No. WNK Verslag No. 302/1/95*, Verslag aan die waternavorsingskommissie deur die Departement of Geologie, Universiteit van Pretoria, South Africa (in Afrikaans).
van Schalkwyk, A., Jordaan, J., and Dooge, N. (1994b). "Erosion of rock in unlined spillways." *Q.71 E.37*, International Commission on Large Dams, Paris.